RSC Advances

PAPER

View Article Online
View Journal | View Issue

Cite this: *RSC Adv.*, 2026, **16**, 5410

Optimization, thermo-oxidative stability, and biological activities of vitamin E-chitosan–TPP nanoformulations

Hussein M. Ali, *[a] Mohamed H. Attia,[a] Wael Mamdouh, [b] Eman N. Rashed[a] and Isra H. Ali[cd]

Enhancing stability is a crucial factor in selecting bioactive compounds in most applications, while encapsulation techniques have proven to be a promising solution. Despite the critical applications of α-tocopherol (α-TQ) in the food and pharmaceutical industries, it is easily degraded by heat and oxidized by various oxidants in cells and foods; therefore, its more stable but less active acetate form (α-TQA) is commonly utilized. This study first optimized the preparation of the chitosan (CS) α-TQ nanoemulsion (α-TQ/CS–TPP/NE) using response surface methodology (RSM), achieving a minimum particle size of 278.1 nm; nanoparticles were also prepared and characterized by IR, TEM, and thermal analysis. Second, the chitosan nanoformulation exhibited greater thermal and oxidative stability against H_2O_2 and HOCl (>99%) than the precursors, α-TQ (68.62% and 22.22%) and α-TQA (86.86% and 26.44%), after 4 days. The nanoformulations also enhanced antioxidant activity against DPPH and hydroxyl radicals, as well as the reducing power, whereas α-TQA and its nanoparticles did not demonstrate antioxidant activity. Third, the kinetics of tocopherol release in different solvents were investigated and found to follow first-order kinetics, with diffusion as the main mechanism. Fourth, the nanoemulsion demonstrated effective applications in providing oxidative stability for edible oils at elevated temperatures, reducing oil oxidation by more than 85% upon heating at 100 °C for 5 hours. Fifth, α-TQ/CS–TPP/NE could enhance its anticancer activity against breast cancer (MCF-7). The increased thermo-oxidative stability, antioxidant activity, oil stabilization, and anticancer activity make α-TQ/CS–TPP/NE a valuable option as a dietary supplement or food additive.

Received 14th August 2025
Accepted 15th January 2026

DOI: 10.1039/d5ra06012e

rsc.li/rsc-advances

1 Introduction

Among the four natural tocopherol isoforms (α, β, γ, and δ), α-tocopherol (α-TQ) is the most common and active form found in foods and, consequently, in human tissues; therefore, it is regarded as the active vitamin *E* tocopherol isoform.[1–3] Due to its inherent phenolic structure and fully substituted aromatic ring with electron-donating groups, it exhibits potent antioxidant activity, providing protection against lipid peroxidation, which serves as a primary function in plants.[4,5] It also offers valuable health benefits for humans and is commonly used as a pharmaceutical supplement to protect against various chronic diseases.[1,2] However, α-TQ is highly susceptible to oxidation by environmental factors and reactive oxygen species (ROS), *e.g.*, hydrogen peroxide,[6] singlet oxygen,[7] and superoxide anion;[8] hydroxyl radical, perhydroxyl radical,[9] and peroxynitrite ($ONOO^-$) radical.[10]

Consequently, due to its low stability and sensitivity to oxidation, the typical α-TQ form used in the food and pharmaceutical industries is the acetate form (α-TQA); however, this form lacks antioxidant activity and must be hydrolyzed first to become biologically active.[3,11]

Hydrogen peroxide is one of the major reactive oxygen species (ROS) primarily formed in the mitochondria, followed by the chloroplasts. Its main adverse effect is the production of the hydroxyl radical, one of the most reactive ROS in cells, through the abstraction of an electron from either a ferric ion (Fenton reaction) or superoxide anion (Haber–Weiss reaction), which explains the occurrence of vitamin *E* in the highest concentration in the mitochondrial inner membrane.[12,13] Hypochlorous acid is a potent oxidant formed in the neutrophils by the action of myeloperoxidase on hydrogen peroxide and chloride ion. It is used to protect cells from invading bacteria and pathogens, but its accumulation results in severe

[a]*Agricultural Biochemistry Department, Faculty of Agriculture, Ain-Shams University, P. O. Box 68, Hadayek Shoubra, Cairo 11241, Egypt. E-mail: Hussein_galaleldeen@agr.asu.edu.eg; mohamed_aboudoma@agr.asu.edu.eg; emannasreldeen@agr.asu.edu.eg*

[b]*Department of Chemistry, School of Sciences and Engineering, The American University in Cairo (AUC), AUC Avenue, P. O. Box 74, New Cairo 11835, Egypt. E-mail: wael_mamdouh@aucegypt.edu*

[c]*Department of Pharmaceutics, Faculty of Pharmacy, University of Sadat City, P. O. Box 32897, Sadat City, Egypt. E-mail: isra.ali@fop.usc.edu.eg*

[d]*Department of Cardiovascular Medicine, Mayo Clinic, Rochester, MN, USA*

adverse effects, as it reacts rapidly with various biological molecules; more importantly, no enzymatic mechanism is known to remove this oxidant, as with hydrogen peroxide.[14]

Encapsulation is an effective method for protecting bioactive compounds, especially sensitive antioxidants, from oxidative stress in the food and pharmaceutical industries. Molecular inclusion complexation involves trapping the bioactive guest molecule within a host polymer through physicochemical interactions, such as hydrogen bonding, hydrophobic interactions, or van der Waals forces.[15] Among the various polymers, chitosan has unique properties. It is a nontoxic, biodegradable, naturally derived polymer resulting from the partial deacetylation (>50%) of chitin, which consists of acetylated D-glucosamine molecules linked by (β-1 → 4) glycosidic bonds. Additionally, its free amino group has basic properties and gives chitosan a cationic structure at acidic or physiological pH; the amine and hydroxyl groups also enhance the solubility of hydrophobic guests and enable interaction with various materials.[16–18]

Although α-tocopherol was encapsulated by chitosan previously,[19–21] as far as we know, no report has optimized the preparation using response surface methodology (RSM); besides, no work has compared the oxidative stability against ROS, antioxidant activity, oil stabilizing activity, and anticancer activity of the encapsulating active α-TQ with the commercial inactive α-TQA. Therefore, this work hypothesizes that encapsulating the unstable but active form of tocopherols, α-TQ, with chitosan–TPP can improve its stability against ROS and heat; additionally, encapsulation allows for the control of α-TQ release in the media. The effects of encapsulation on enhancing the antioxidant activity, anticancer activity, and thermal stability of edible oil were explored and compared with the inactive tocopherol form, α-TQA, and its complex; therefore, the present research was designed as follows: first, to optimize the preparation of α-TQ/CS–TPP/NE for both the free (α-TQ) and acetate (α-TQA/CS–TPP/NE) forms. Subsequently, characterization was performed using IR, thermal analysis, ZetaSizer, and transmission electron microscopy (TEM). Second, the study examines the oxidative stability of the prepared nanochitosan complexes and their precursors, α-TQ and α-TQA, against reactive oxygen species (ROS), including hydrogen peroxide and hypochlorous acid. Additionally, their antioxidant activity and tocopherol release performance were evaluated. Finally, the applications of the prepared nanoformulation in stabilizing edible oil against oxidation at elevated temperatures, as well as improving the anticancer activity of tocopherols, are investigated.

2 Experimental sections

2.1. Chemicals and instrumentation

α-Tocopherol (α-TQ, $C_{29}H_{50}O_2$, MW 430.71) was obtained from Sigma Co. α-Tocopheryl acetate tablets (α-TQA, $C_{31}H_{52}O_3$, MW 472.74) were purchased from Pharco-Pharmaceuticals Co. Low MW chitosan (CS, *N*-acetyl-β (1→4) D-glucosamine, 200–250 kDa) was extracted from Pandalus borealis with a deacetylation degree of 89.9%, and was manufactured by Primex ehf, Oskarsgata, Siglufjordur, Iceland. Tween 80 (Polysorbate 80, hydroxyl value 65–80) was purchased from Pioneers for Chemicals (Piochem), Giza, Egypt. Glacial acetic acid (99.7%), absolute ethanol (99%), phosphate-buffered saline (PBS, pH 7.4), and cellulose dialysis membrane (cut-off 12 000 MW) were obtained from Sigma-Aldrich, Taufkirchen, Germany. DPPH (2,2-Diphenyl-1-picrylhydrazyl, $C_{18}H_{12}N_5O_6$, MW 394.32) was purchased from Sigma-Aldrich. Sodium tripolyphosphate (TPP, Na5O10P3, MW 367.86), trichloroacetic acid (TCA, MW 163.39), and sodium hypochlorite solution (NaOCl, 15.18 mM; available chlorine 4.0–6.0%, MW 74.44) were purchased from Advent Chembio Pvt. Ltd. Hydrogen peroxide (30%, 8.820 M) was sourced from Research-Lab Fine Chem. Ferric chloride ($FeCl_3 \cdot 6H_2O$, MW 270.30, 99%) and potassium ferric cyanide ($K_3Fe(CN)_6$, MW 329.24, 99%) were from Alpha Chemika, India, and Belami Fine Chemicals Pvt. Ltd, respectively. Thiobarbituric acid (TBA) ($C_4H_4N_2O_2S$, MW 144.15) was obtained from Advent Chembio PVT. Ltd, India.

The homogenizer used was Daihan, Korea. The probe sonicator employed was LC 60/H^{-1}, Elma, Germany. UV-vis spectra were recorded with a Thermo Fisher Evolution 300 spectrometer over a scan range of 200–600 nm. IR spectra were measured using an FT-ATR-IR model Bruker Vertex 80/80 V in the range of 4000–400 cm^{-1}. The ZetaSizer used for analyzing particle size and surface charge was Malvern, UK. The Transmission Electron Microscope used was a JEOL TEM-2100F.

2.2. Preparation and optimization of nanoemulsions and nanoparticles of CS/α-TQ and CS/α-TQA

2.2.1. Screening for experimental design factors. Both (O/W) α-TQ-in-water (α-TQ/NE) and α-TQ-chitosan–TPP-in-water (α-TQ/CS–TPP/NE) nanoemulsions (NEs) were prepared following a previously reported methodology with minor modifications.[22,23] Screening and optimization were conducted to encapsulate α-TQ in a chitosan–TPP nanoemulsion (α-TQ/CS–TPP/NE), after which the optimized conditions were applied to the α-TQA nanoemulsion (α-TQA/CS–TPP/NE). Initially, a coarse microemulsion was prepared by adding α-TQ dropwise to an aqueous phase containing Tween 80, a nonionic surfactant, while stirring at room temperature. The coarse emulsion was further homogenized at 10 000 rpm for 10 minutes using a homogenizer to reduce the size of the oil droplets forming the microemulsion. This constitutes the primary stage of α-TQ nanoemulsion (α-TQ/NE) preparation. Similarly, the initial stage of preparing the chitosan-coated α-TQ microemulsion followed the previously mentioned steps. The aqueous phase contained chitosan dissolved in 1% glacial acetic acid, and a sodium tripolyphosphate (TPP) solution was added dropwise as a crosslinking agent during the homogenization step.

Afterward, both pre-formulated microemulsions were sonicated using a probe sonicator to minimize the oil droplets that formed the corresponding NEs. The sonication cycle lasted 10 minutes (10 seconds on, followed by 5 seconds off) at 20 kHz and 400 W. The sonication process was performed while keeping the samples in an ice bath to prevent overheating, thereby preserving sample stability.[24] Finally, both α-TQ/NE and

α-TQ/CS–TPP/NE were stored at 4 °C under refrigeration until needed for further characterization.

Chitosan concentration (% w/v), the oil-to-aqueous phase ratio, and the TPP : CS ratio were screened by preparing 12 different nanoformulations to identify reliable factors that can be tailored, as described in the Experimental Design Section. The twelve formulated nanoformulations were investigated for their size (nm), polydispersity index (PDI), and surface charge (mV), as presented in Table S1.

2.2.2. Experimental design. The Box-Behnken design (BBD) with Design-Expert software was used to predict the optimal factor levels for preparing the desired α-TQ/CS–TPP/NE nanoemulsions. The same steps outlined earlier in Section 2.2.1 were used to prepare various formulations, with several independent factors affecting the properties of the developed nanoemulsions, including CS solution concentration (*A*), oil volume (*B*), TPP : Chitosan ratio (*C*), and Tween-80 amount (*D*).

On the other hand, the nanoemulsion droplet size (nm), polydispersity index (PDI), and surface charge (mV) were identified as the dependent variables (responses) in the experimental design. The low and high values were established based on preliminary screening. For example, the required amounts of chitosan were dissolved in 1% acetic acid to prepare 0%, 1%, and 2% w/v chitosan solutions. Additionally, the oil volumes tested (mL) were 1, 2, and 3 mL. The TPP : chitosan ratios examined were set at 0 : 1, 0.1 : 1, and 0.2 : 1. The amounts of Tween 80 evaluated (mg) were 300, 400, and 500 mg. The Box–Behnken design generated 27 formulations for preparation and assessment, as indicated in Table 1. Subsequently, both numerical and graphical optimizations were performed to identify the formulation with the highest desirability based on the value of each response. Finally, the models were validated by calculating the Bias % using the following equation.[25]

$$\text{Bias}(\%) = \left(\frac{(\text{Predicted value} - \text{Experimental value})}{\text{Experimental value}}\right) \times 100$$

The optimized method was as follows: a chitosan solution (CS, 1.612%) in 1% acetic acid was prepared. In a beaker, 339.786 mg of Tween-80 and 8.772 mL of CS solution were magnetically stirred for 3 minutes. Afterward, 1.228 mL of α-TQ or α-TQA (density 0.95 g mL^{-1}) was added dropwise to prepare an α-TQ (270.9 mM) or α-TQA (246.9 mM) emulsion to a final volume of 10 mL. The mixture was homogenized with a homogenizer (10 000 rpm) for 10 minutes, during which a TPP solution (1.0 mL, 0.028 mg mL^{-1} in distilled water) was added; the CS : TPP ratio was 1 : 0.199. The emulsion was then sonicated using a probe sonicator for 10 minutes.

Nanoparticles of α-TQ (α-TQA/CS–TPP/NPs) and α-TQA (α-TQA–CS–TPP/NPs) were produced by freeze-drying the nanoemulsion. The loading capacity (LC) was assessed by extracting tocopherol from the complex (20–35 mg) using ethanol extraction with ultrasonication. The resulting clear solution was adjusted to a final volume of 100 mL with ethanol, and the absorbance was measured at 292 nm for α-TQ and 287 nm for α-TQA; spectra are presented in Fig. S1. The results are the mean of triplicate. Tocopherol concentration was determined from the prepared standard curves that yielded the following equations:

$$A_{292\text{nm}}\ (\alpha\text{-TQ}) = 0.020 + 0.090\ [\alpha\text{-TQ}]_{\text{mg/100mL}}\ (\text{EtOH},\ R^2\ 0.969)$$

$$A_{287\text{nm}}\ (\alpha\text{-TQA}) = -0.011 + 0.045\ [\alpha\text{-TQA}]_{\text{mg/100mL}}\ (\text{EtOH},\ R^2\ 0.999)$$

$$\text{LC} = (\text{weight of recovered } \alpha\text{-TQ or } \alpha\text{-TQA/NPs' weight}) \times 100$$

2.3. Thermal analysis

Thermogravimetric analysis was performed using the TA SDT Q600 instrument under nitrogen. The operating conditions were: initial temperature, 50 °C; final temperature, 550 °C; and heating rate, 10 °C min^{-1}. Samples (10 mg) were placed in open crucibles for thermogravimetry (TG) and differential thermogravimetry (DTG) measurements. In Differential Scanning Calorimetry (DSC), sealed pans with lids containing a hole pierced with a thick pin were used. The degradation peaks were observed in the DTG thermograph, and the onset temperatures were measured at the intersection of the extrapolated baseline before transition with a tangent to the defective peak.

2.4. Transmission Electron Microscope (TEM)

The prepared nanoemulsions were morphologically investigated using a Transmission Electron Microscope (TEM-2100F, JEOL, USA). A drop of each diluted nanoemulsion was placed separately onto a copper TEM grid and then stained with phosphotungstic acid for sample preparation. The prepared samples were subsequently examined under TEM to assess the shape and features of the nanodroplets.

2.5. Tocopherol oxidative stability

The oxidative stability of α-TQ and α-TQ/CS–TPP/NPs was examined against various reactive oxygen species (ROS). Aqueous solutions containing 74.147 mM H_2O_2 and 147.07 μM α-TQ (dissolved in ethanol) were incubated in closed tubes covered with aluminum foil at 25 °C. Absorbance was measured at 292 nm at each interval, and tocopherol concentration was derived from a standard curve. In other tubes, each containing H_2O_2 (74.147 mM) and α-TQA/CS-TPP/NPs at the same α-TQ concentration (147.07 μM), incubation was conducted similarly. At each interval, three tubes were centrifuged, and each was extracted three times with ethanol, resulting in a final volume of 15 mL. The tocopherol concentration was determined as previously described. Stability against HOCl was assessed in the same manner, but at pH 6.2 (10 mL) with concentrations of 208.53 μM (α-TQ or α-TQA) and 1600 μM (HOCl). Results are expressed as the mean percentage of the remaining tocopherol in triplicate (±SD).

2.6. Antioxidant activities

The scavenging activity of tocopherols (α-TQ, α-TQ/CS–TPP/NPs, α-TQA, and α-TQA/CS-TPP/NPs) was assessed against DPPH and hydroxyl radicals. The reducing potential towards ferricyanide ions was also investigated. All experiments were conducted in

Table 1 Preparation and optimization of CS/α-TQ NE experimental runs

	Independent factors				Dependent variables		
Run	X1: chitosan conc (w/v%)	X2: oil volume (mL)	X3: TPP : chitosan ratio	X4: Tween 80 (mg)	Y1: size (nm)	Y2: PDI	Y3: charge (mV)
	0	2	0.2	400	2983.67	0.308	−17.76
2	1	1	0.1	500	487.3	0.536	30.80
3	0	2	0	400	3718	0.181	−23.73
4	2	3	0.1	400	994.767	0.793	31.13
5	1	1	0.2	400	489.967	0.456	36.13
6	2	2	0	400	665.567	0.096	40.10
7	0	1	0.1	400	1551	0.478	−14.43
8	1	3	0.1	500	1522.33	0.334	32.46
9	1	2	0.1	400	548.733	0.124	30.60
10	1	2	0.1	400	844.367	0.199	29.73
11	0	2	0.1	500	4133.33	0.206	−9.17
12	1	2	0.1	400	996.967	0.233	30.23
13	2	1	0.1	400	1151.03	0.128	32.23
14	1	2	0	500	835.533	0.155	32.6
15	1	2	0.2	500	825.733	0.440	36.96
16	2	2	0.1	500	487.6	0.278	29.83
17	2	2	0.2	400	453.167	0.094	40.86
18	1	1	0.1	300	315.133	0.190	33.53
19	1	1	0	400	1837	0.262	27.96
20	0	2	0.1	300	3299	0.486	−19.73
21	0	3	0.1	400	3568.67	0.234	−10.5
22	1	2	0.2	300	799.1	0.117	29.53
23	2	2	0.1	300	1010.93	0.493	38.3
24	1	3	0	400	665.167	0.145	31.9
25	1	2	0	300	1149.63	0.346	36.03
26	1	3	0.2	400	2077	0.273	28.43
27	1	3	0.1	300	1205.33	0.279	31.3

triplicate (±SD). The amounts of complexes containing the required tocopherol were calculated based on the loading capacity of each complex.

2.6.1. DPPH scavenging activity. The scavenging of DPPH (2,2-diphenyl-1-picrylhydrazyl) was determined as described previously.[26,27] Briefly, a 0.004% methanolic DPPH solution (0.1 mM) was freshly prepared. To a 2.0 mL DPPH solution in a cuvette, various concentrations of α-TQ or α-TQA (1.0 mL) dissolved in EtOH were added, resulting in final concentrations of 3.68, 14.71, 22.06, 36.77, 73.63, and 110.3 μM. In the control experiment, EtOH was added instead of the tocopherols. Nanoparticles with the same tocopherol concentration were used. Absorbance was measured after 5 minutes at 517 nm against a blank containing no DPPH. The DPPH inhibition was calculated using the following equation:

$$\%\ \text{DPPH inhibition} = ((A_{\text{control}} - A_{\text{exp}})\ /A_{\text{control}}) \times 100$$

where A_{control} and A_{exp} are the absorbance of the control and experiment, respectively.

2.6.2. Hydroxyl radical scavenging activity. The hydroxyl radical scavenging activity was determined using the method of,[28] with modifications as described. In stoppered vials, 2.0 mL of $FeSO_4$ (4.5 mM), 1.0 mL of H_2O_2 (0.25%), and 1.0 mL of α-TQ or α-TQA (or their nanoparticles) were mixed, resulting in final tocopherol concentrations of 0.53, 0.88, 1.23, 1.94, and 2.65 mM; EtOH served as a control. The mixtures were incubated for one hour at 25 °C, after which 1.0 mL of salicylic acid (4.51 mM) was added and incubated for an additional 10 minutes. The mixture was centrifuged at 2000 rpm for 10 min. The absorbance was measured at 510 nm against a blank with no H_2O_2. The inhibition percentage of hydroxyl radical was calculated as follows:

$$\%\ \text{OH radical inhibition} = (A_{\text{exp}})/A_{\text{control}}) \times 100$$

2.6.3. Reducing power. Reducing power was estimated using a modified method of Oyaizu.[29] Briefly, 3.0 mL potassium ferricyanide (1%) was added to 50 mL of various ethanolic α-TQ or α-TQA concentrations (or equivalent NPs); the mixture was incubated at 50 °C for 20 min. TCA (3.0 mL, 10%) was added with shaking, followed by 1.5 mL of ferric chloride (0.1%). The absorbance was recorded at 700 nm against a blank with EtOH instead of tocopherols. The increase in the developed blue color was used as an indicator of the tocopherol reduction potential.

2.7. Tocopherol release

The tocopherol release experiment was conducted by suspending 10.53 mg α-TQ/CS–TPP/NPs (containing 19.261 μmol α-TQ) or 13.10 mg α-TQA/CS-TPP/NPs (containing 22.70 μmol α-TQ) in 2 mL of solvent (EtOH or CH_2Cl_2) in an Eppendorf vial covered with dialysis tubing, which was then placed in a Falcon tube containing 13 mL of solvent. At each interval, 3 mL was removed

for absorbance measurement and replaced with fresh solvent. Absorbance was measured for α-TQ and α-TQA in ethanolic solutions at 292 and 287 nm, and in methylene chloride solutions at 295 and 285 nm, respectively, as exhibited in their spectra (Fig. S1). Each experiment was performed in triplicate (±SD).

Various kinetic release models were applied, including the first order, Higuchi, and Hixson-Crowell models[30–32] using the below linear regressions, respectively:

$$\text{Ln [retained α-TQ (α-TQA), μmol]} = \ln[\text{initial amount, μmol}] - kt$$

$$\text{Ln [released α-TQ (α-TQA), μmol]} = \ln k_H + 1/2 \ln t$$

$$\text{Ln [retained α-TQ (α-TQA), μmol]} = \ln[\text{initial amount, μmol}] - 3k_{H-C} \times t$$

where t is the interval time (min), k is the first-order rate constant, k_H is the Higuchi correlation constant, and k_{H-C} is the Hixson–Crowell constant.

The concentrations of α-TQ and α-TQA in methylene chloride were determined using equations derived from standard curves prepared in this solvent. Their spectra in different solvents are shown in Fig. S1.

$$A_{295nm}\ (\alpha\text{-TQ}) = -\ 0.0065 + 0.0673\ [\alpha\text{-TQ}]_{mg/100mL}\ (CH_2Cl_2,\ R^2\ 0.999)$$

$$A_{285nm}\ (\alpha\text{-TQA}) = 0.0178 + 0.0424\ [\alpha\text{-TQA}]_{mg/100mL} + (CH_2Cl_2,\ R^2\ 0.999)$$

2.8. Oil thermo-oxidative stability by tocopherol nanoformulations

In a Petri dish, oil (25 mL) and a sample (α-TQ, α-TQA, α-TQ/CS–TPP/NE, or α-TQA/CS–TPP/NE) containing 110.29 μmol (0.19% w/v) tocopherol were added, and the mixture was shaken until well mixed in a dark room. Each sample was prepared in triplicate. Dishes were incubated at 100 °C, and 1 mL was drawn from each dish at each interval for MDA determination.[33] An oil sample (1 mL) and TBA (3.0 mL, 0.5% in 20% TCA) were mixed by vortexing in a screw test tube with a screw cap. Tubes were heated in a water bath for 30 minutes and then cooled in the refrigerator for 10 minutes. Absorbance was recorded at 532 nm for each sample. The percentage of MDA production was expressed as the mean of triplicate (±SD) and calculated according to the following equation:

$$\%\ \text{MDA production} = ((A_s - A_o)/(A_c - A_o)) \times 100$$

A_s: absorbance of oil + tocopherol at 100 °C after a particular period. A_c: absorbance of oil at 100 °C after the same period. A_o: absorbance of oil without heating.

2.9. Anticancer activity of α-tocopherols and their nanoemulsions

MCF-7: Breast Adenocarcinoma was obtained from Nawah Scientific Inc. (Mokatam, Cairo, Egypt). Cells were maintained in DMEM media supplemented with 100 mg mL^{-1} of streptomycin, 100 units/mL of penicillin, and 10% heat-inactivated fetal bovine serum in a humidified atmosphere with 5% (v/v) CO_2 at 37 °C.

Cell viability was assessed using the SRB assay.[34] Aliquots of 100 μL of cell suspension (5×10^3 cells) were placed in 96-well plates and incubated in complete media for 24 hours. Cells were treated with another 100 μL aliquot of media containing the tocopherol sample at various concentrations. Afterward, cells were fixed by replacing the media with 150 μL of 10% TCA and incubated at 4 °C for 1 hour. The TCA solution was removed, and the cells were washed five times with distilled water. Aliquots of 70 μL of SRB solution (0.4% w/v) were added, and the mixture was incubated in the dark at room temperature for 10 minutes. The plates were washed three times with 1% acetic acid and allowed to air-dry overnight. Next, 150 μL of TRIS (10 mM) was added to dissolve the protein-bound SRB stain; the absorbance was measured at 540 nm using an Infinite F50 Microplate Reader (TECAN, Switzerland). Absorbance was used to quantify cell cytotoxicity; results are the mean of triplicate measurements.

3 Results and discussion

3.1. Preparations of tocopherol–chitosan–TPP nanoformulations

The preparation of α-TQ/CS–TPP/NE was optimized for minimizing the emulsion particle size (nm) and polydispersity index (PDI) while maximizing the particle surface charge (mV). Twelve preliminary experiments were conducted to determine the coarse range for each preparation-dependent variable, specifically CS concentration (w/v%), oil volume (mL), aqueous phase volume (mL), and TPP : CS ratio. Afterwards, a design of 27 experimental runs was executed to reach the optimal preparation conditions.

3.1.1. Screening the preparation factors. The results of the twelve preliminary experiments (Table S1) highlight the significant impact of these factors on the measured responses of the nanoemulsion, including particle size, PDI, and surface charge. A comparison of each of the three consecutive runs revealed that increasing the oil volume led to the formation of nanoemulsions with larger particle sizes. However, raising the concentration of chitosan decreased particle sizes. Furthermore, comparing runs 1–6 with their corresponding runs 7–12 indicates that the addition of TPP resulted in a noticeable reduction in particle size, underscoring the role of TPP in crosslinking and compacting the polymeric network of chitosan.

Lower PDI values below 0.3 indicate good size uniformity. The lowest PDI values observed were 0.119 (run 10) and 0.128 (run 4), which were found in a nanoemulsion with high chitosan and low oil concentrations. Additionally, the incorporation of TPP consistently reduced the PDI, resulting in a more monodisperse system, as shown by comparing runs 1–6 with runs 7–12.

3.1.2. Optimization of the nanoformulation preparation. The preliminary study suggests extending the CS level (0–3%), the oil volume (1–3 mL), and the TPP : CS ratio (0–0.2) in the

optimization experiment. Additionally, the factor of the added amount of Tween-80 (300–500 mg) was examined. The Box-Behnken design, with four factors each having three levels, recommended 27 experiments with different combinations of the factor levels, as detailed in Table 1. The results demonstrated that all dependent variables adhered to a quadratic model with good predictive capability, as all adequate precision values exceeded 4. Furthermore, the adjusted R^2 and predicted R^2 values for both size and surface charge were high and closely similar (Table S2).

Designing nanoformulations with minimal size is crucial because increased surface area enhances loading capacity.[25,35] The response surface methodology (RSM) curve (Fig. 1) showed that the TPP : CS ratio (C) significantly influences the particle size, with the particle size decreasing noticeably due to improved crosslinking efficiency. This confirms the essential role of electrostatic interactions between the polyanionic TPP and the polycationic chitosan chains during nanoparticle formation, consistent with previous studies.[36] For instance, minimal crosslinking at a low TPP : CS ratio ($C = 0$) resulted in the formation of a loose polymeric network, leading to larger droplets with greater size variability due to water and oil penetration. However, as the ratio increases, crosslinking begins to compact the polymer matrix, reducing oil droplet expansion and enhancing the stability of the developed nanoemulsions.

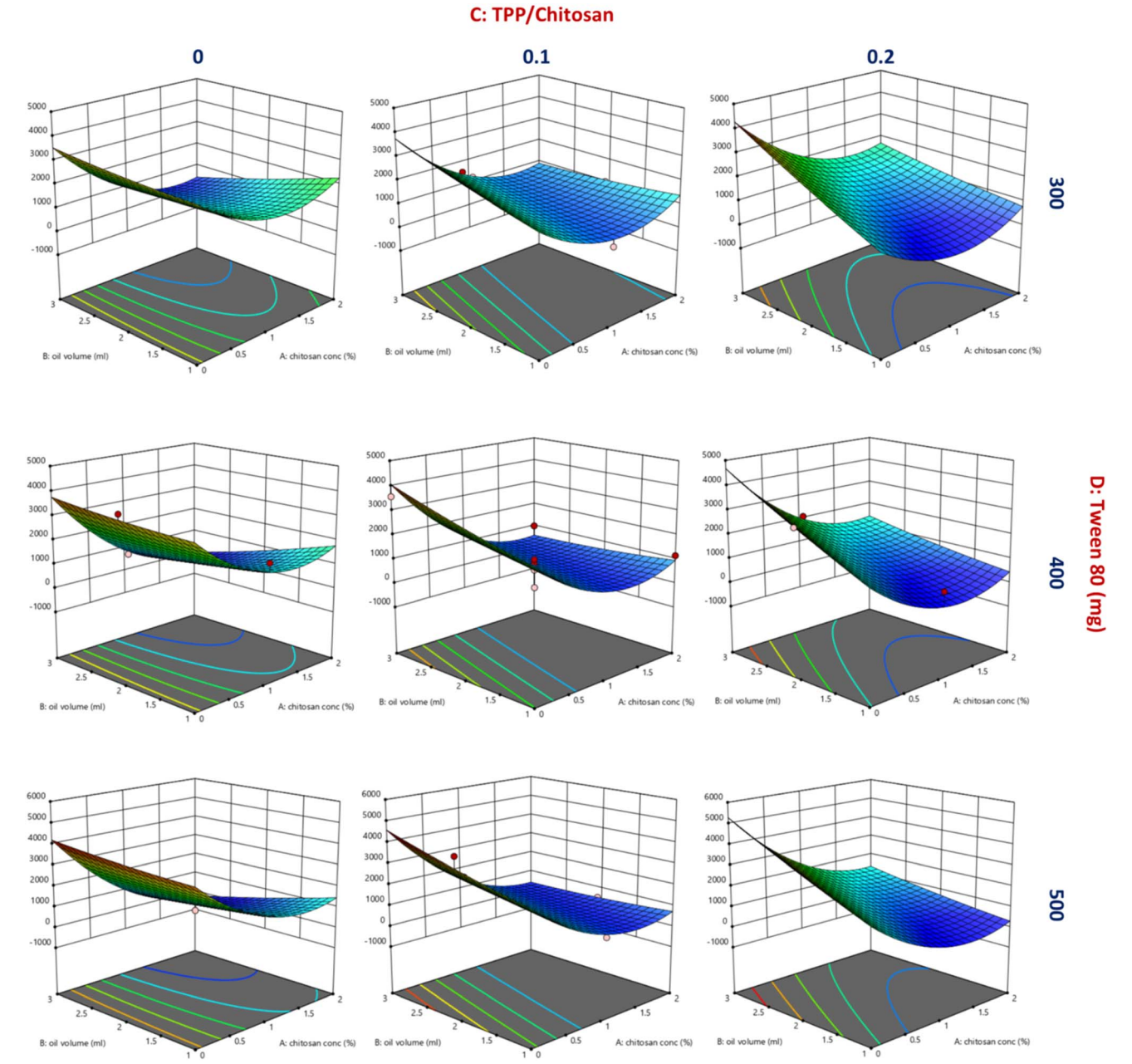

Fig. 1 RSM of the effect of CS concentration (A) and oil volume (B) on particle size (Y1) under different conditions of TPP : chitosan ratio (C) and tween 80 (D).

Although the surfactant Tween-80 (D) aids proper emulsification and reduces particle size, excessive amounts can interfere with TPP-chitosan interactions, leading to the opposite effect and destabilizing the system.

RSM plots (Fig. S2), Tables 1 and S1 indicate that increasing the TPP : CS ratio (C) decreased the PDI by enhancing particle uniformity through increased crosslinking. Conversely, higher Tween-80 concentrations led to a dramatic increase in PDI values, particularly at elevated C levels, confirming that excess surfactant can destabilize the system. The middle Tween-80 concentration (D = 400 mg) yielded the most stable nanoemulsions. Additionally, low CS concentrations ($A \approx 0.5\%$) led to high PDI values due to insufficient polymer stabilization. Moreover, increasing oil volume (B) led to higher PDI values due to the formation of larger, less stable droplets.

The surface charge (zeta potential) RSM plots (Fig. S2), Tables 1 and S1 demonstrate that increasing the CS concentration (A) remarkably enhances the intensity of positive surface charge, underscoring the role of CS as a cationic stabilizer. Increasing oil volume (B) also led to a slight increase in charge. A higher charge intensity is deemed essential for maintaining the stability of the prepared nanoformulations.[25,37] Additionally, a higher TPP : CS ratio (C = 0.2) strengthened electrostatic interactions between positively charged amino groups on chitosan chains and negatively charged phosphate groups on TPP molecules, leading to greater system stability. Conversely, increasing the amount of Tween-80 caused a slight decrease in surface charge intensity. This may be due to the non-ionic nature of Tween-80, which can partially shield the chitosan positive charge, thereby weakening electrostatic repulsion and leading to aggregation. Therefore, optimizing the TPP : CS ratio, Tween-80 content, and CS concentration is crucial for maintaining stabilized, homogeneously dispersed nanoemulsions and preventing aggregation.

The numerical and graphical optimization results are respectively illustrated in Fig. 2a as a desirability plot and Fig. 2b as an overlay plot. The former plot shows the highest desirability value of 1.0 in the red zone, confirming that the optimized independent factors yield the best multiple response variables (smallest particle size, lowest PDI, and highest surface charge). This optimal zone indicates that the optimal formula has been achieved with a chitosan concentration of 1.612% w/v and an oil volume of 1.22 mL. On the other hand, the contour lines show that moving away toward either lower chitosan concentrations or higher oil volumes has led to a noticeable reduction in the desirability score. Moreover, the overlay plot confirms the graphical and numerical optimization results, in which the yellow region meets all specified constraints, including the desired ranges for size, PDI, and zeta potential. However, the grey area represents the regions where one or more constraints have not been satisfied.

Accordingly, this analysis revealed that the optimal conditions are a chitosan concentration of 1.612% w/v and an oil volume of 1.228 mL, with the TPP : CS ratio maintained at 0.199 and Tween-80 at 339.80 mg (Fig. 2 and Table 2). At the same time, the predicted responses are particle size of 202.532 nm, PDI of 0.085, and surface charge of 43.068 mV (Fig. 2 and Table 2); the factor coefficients and their significances for the predicted values are listed in Table S3. α-TQ/CS–TPP/NE was then freshly prepared using the optimized parameters, and the obtained response values were compared with the predicted values (Table 2). The close agreement between the experimental and predicted values, especially for size and charge, indicates the accuracy and reliability of the proposed model. The loading capacity of α-TQ/CS–TPP/NPs and α-TQA/CS-TPP/NE was also found to be as high as 78.77% and 81.89%, respectively.

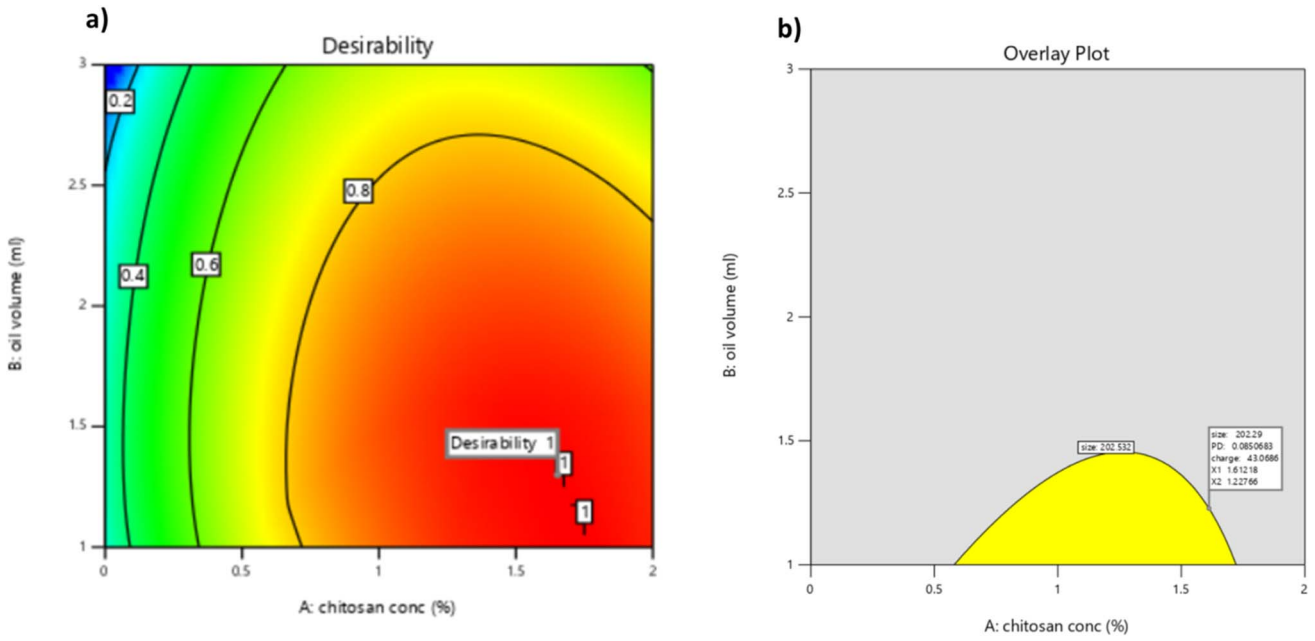

Fig. 2 (a) Desirability plot and (b) overlay plot demonstrating the numerical and graphical optimization results, respectively.

Table 2 The observed (actual) and predicted values of the examined responses for the optimized α-TQ/CS–TPP/NE formulations

Response	Y1: size (nm)	Y2:PDI	Y3: charge (mV)
Observed values	287.1	0.231	44.0
Predicted values	202.532	0.085	43.068
Bias %	29.45	63.20	2.11

3.2. Identification by FT-IR

The IR spectra of TQ and TQA (Fig. 3) show the prominent characteristic peaks at 2907 and 2922 (C–H_{str}), 1452 and 1460 (CH_2 wagging), 1375 and 1376 (CH_3 wagging), and 1253 and 1218 (C–O_{str}) cm^{-1}, respectively. In addition, α-TQA shows a strong C=O_{str} at 1757 cm^{-1}. The complexes of both tocopherols retained these peaks with slight shifts. However, the main difference in IR features between tocopherols and their respective NPs is broadening the peaks in the range 961–1177 cm^{-1} centered at 1080 cm^{-1} because of the additional peaks of the P=O absorbance of the TPP and the C–O_{str} of the chitosan; besides, weak peaks appeared at 935–939 cm^{-1} for the P–O_{str}. Similar chitosan spectra were previously obtained.[38,39] In addition, the formation of hydrogen bonds between the chitosan and each of the two forms of tocopherols is manifested by lowering the wavenumber of the α-TQ hydroxyl group upon complexation from 3461 to 3436 cm^{-1} and slightly reducing the wavenumber of the α-TQA carbonyl group from 1757 to 1755 cm^{-1} (Fig. 3).

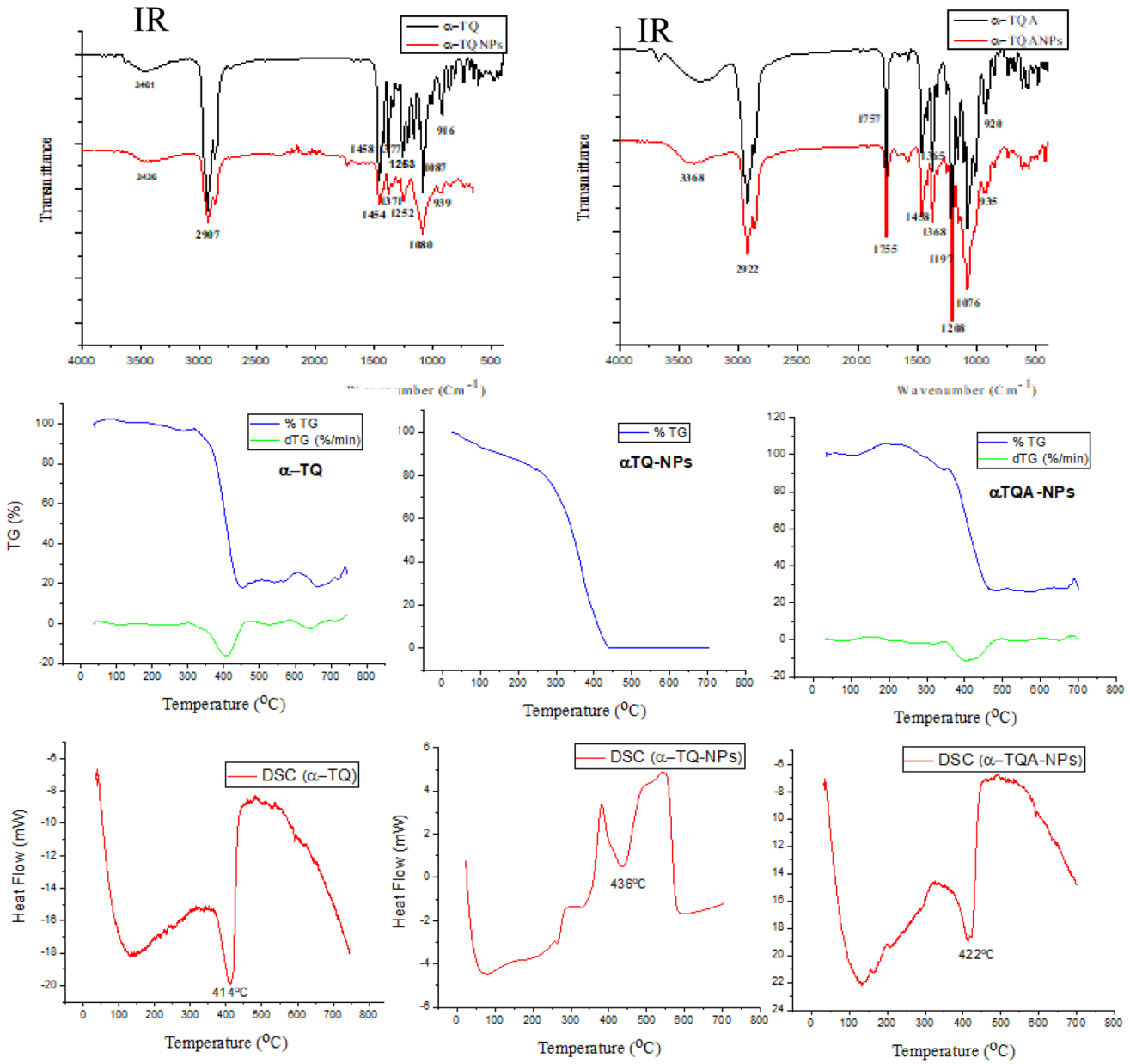

Fig. 3 IR and thermal characterization of α-TQ and α-TQA, and their complexes.

3.3. Thermal stability

Thermal analysis is another technique that indicates the success of the encapsulation process and reveals the thermal stability of tocopherols and their nanoformulation. The thermal stability (TG and DSC) of α-TQ and its nanoparticles (α-TQ/CS–TPP/NPs) was examined and is shown in Fig. 6. The DSC of α-TQ displayed an endothermic peak at 414 °C, while the DTG thermograph indicated that the process involved thermodegradation, leading to a substantial loss of most of the α-TQ weight. α-TQ-NPs showed similar behavior, suggesting that the inclusion of α-TQ provided greater stability, with a degradation peak shifted to 436 °C. Interestingly, chitosan provided greater thermal stability to the active form of α-TQ than our previously studied cyclodextrin and starch complexes.[6,40] The enhanced thermal stability of α-TQ/CS–TPP/NPs is due to the tailored CS-TPP crosslinking framework that surrounds and interacts with α-TQ,[16] thereby providing greater stability than the rigid structures of cyclodextrin and starch.

Similarly, α-TQA showed a previously reported degradation peak at 399 °C,[6,37] whereas the present work revealed greater thermal stability of α-TQA/CS-TPP/NPs, with a degradation peak at 422 °C (Fig. 3). Consequently, nanoformulations demonstrated enhanced thermal stability compared to their precursors, α-TQ and α-TQA. Tocopherol is known for its critical role in stabilizing oils at high temperatures,[41,42] making the α-tocopherol nanoformulation suitable for these applications; thermal analysis was conducted under nitrogen condition. Notably, α-TQ and its nano form displayed greater thermal stability than α-TQA and its nano form, respectively.

3.4. Transmission electron microscopy

TEM micrographs, illustrated in Fig. 4a–d, show non-aggregated spherical nanodroplets, consistent with the size and surface charge results obtained from DLS measurements (Section 3.1). Chitosan (CS) is adsorbed at the oil–water interface, forming an entire and compact positively charged shell after being ionically crosslinked with TPP through the ionotropic gelation technique. Hence, this positively charged shell induces electrostatic repulsion between the nanodroplets, thereby hindering their coalescence and consequently improving PDI uniformity. This, in turn, helps increase kinetic stability and facilitates cellular uptake compared to other anisotropic shapes. Our obtained non-aggregated spherical nanodroplets are found to agree with previously reported chitosan-coated nanoemulsions that demonstrate enhanced stability.[43–45] Overall, TEM results align with the zetasizer measurements, confirming the successful formulation of well-dispersed, spherical NE droplets at the nanoscale, characterized by a narrow PDI and high uniformity.

3.5. Antioxidant activity of tocopherols and their complexes

The antioxidant activities of α-TQ, α-TQA, and their nanoparticle complexes were assessed to compare their effectiveness and to determine whether the nanoformulations influence tocopherol

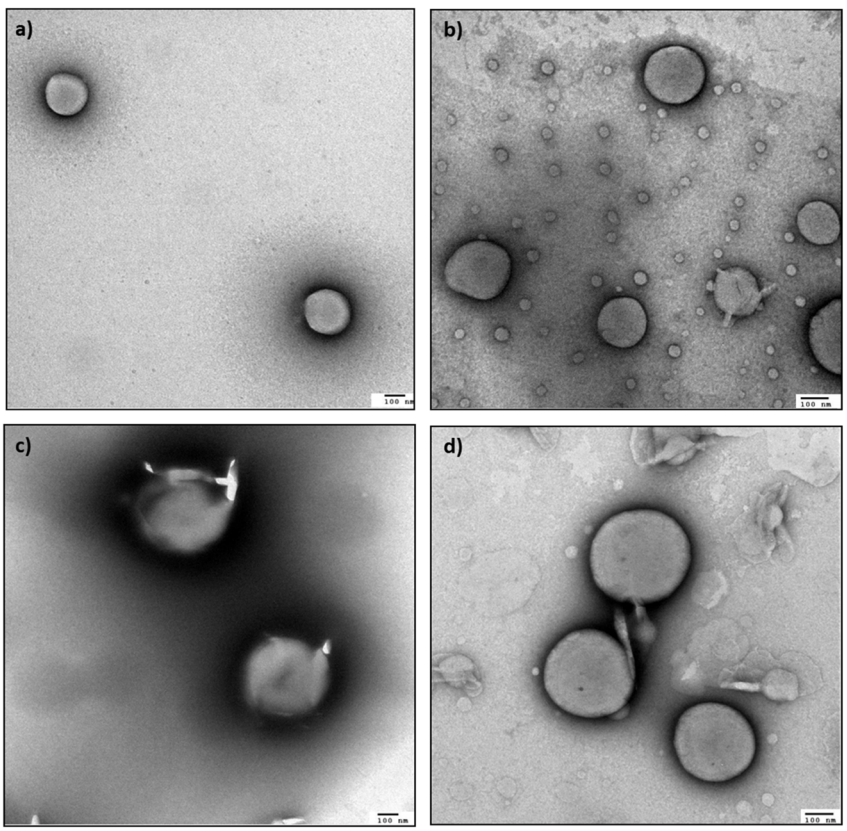

Fig. 4 TEM imaging of (a) α-TQ/NE, (b) α-TQ/CS–TPP/NE, (c) α-TQA/NE, and (d) α-TQA/CS–TPP/NE.

activity. The antioxidant effects were tested against DPPH and hydroxyl radicals. The molar amounts of α-TQ and α-TQA in both free and nanoparticle forms were standardized for each concentration. Results (Fig. 5 and Tables S4–S6) clearly showed that both α-TQA and its nanoparticles lack antioxidant activity against both radicals due to the absence of the phenolic hydroxyl group. The potent antioxidant activity mainly results from the stability of the phenoxyl radical formed by antioxidants and the delocalization of conjugated systems.[46,47] In contrast, α-TQ showed potent activity against both DPPH and hydroxyl radicals. It also appears that α-TQ/CS–TPP/NPs had slightly higher scavenging activity of both radicals compared to α-TQ, which could be linked to the increased surface area and better interaction with free radicals. Besides, it was previously observed that chitosan showed 10.69% scavenging activity against DPPH radicals due to the presence of amine groups, while incorporating 0.1% α-TQ resulted in 97.71% activity;[48] we have also shown that the anilinic group possesses DPPH scavenging activity.[49] This aligns with the present findings, where at 110.3 μM α-TQ (0.05% w/v), and α-TQ/CS–TPP/NPs showed DPPH scavenging activities of 87.06% and 90.82%, respectively (Table S4). Furthermore, some hosts other than chitosan, *e.g.*, niosomes, did not enhance α-TQ activity against the DPPH radical.[50]

Additionally, the reducing power against ferric ions followed a similar trend, with α-TQA and its nanoformulation expressing

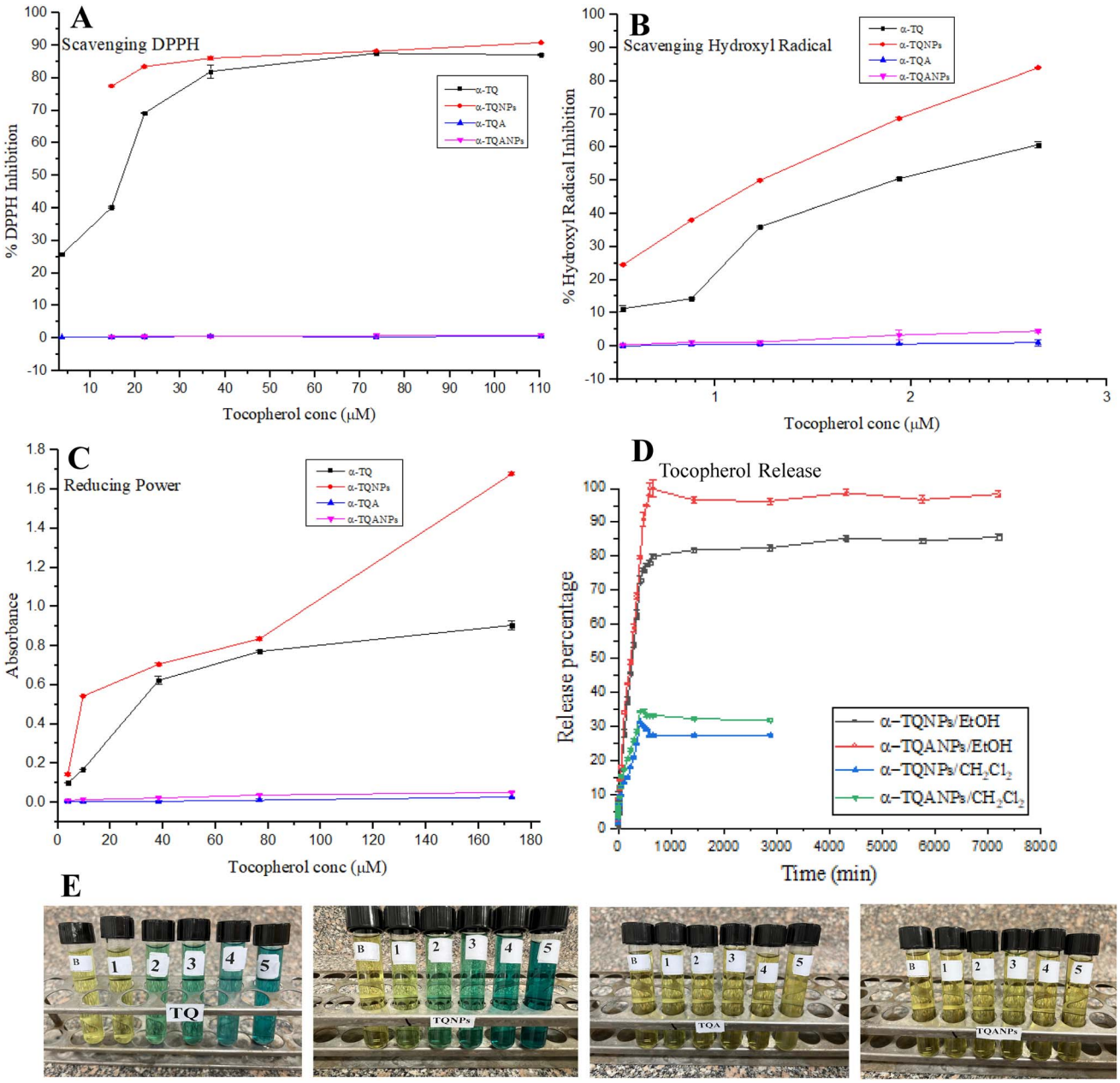

Fig. 5 Antioxidant activities (A and B), the reducing power (C), and the release from nanoparticles in different solvents (D) of tocopherols. Reducing power tubes (control B and 1–5) in ascending order of concentrations (E). Results are means of triplicate, with error bars representing the standard deviations.

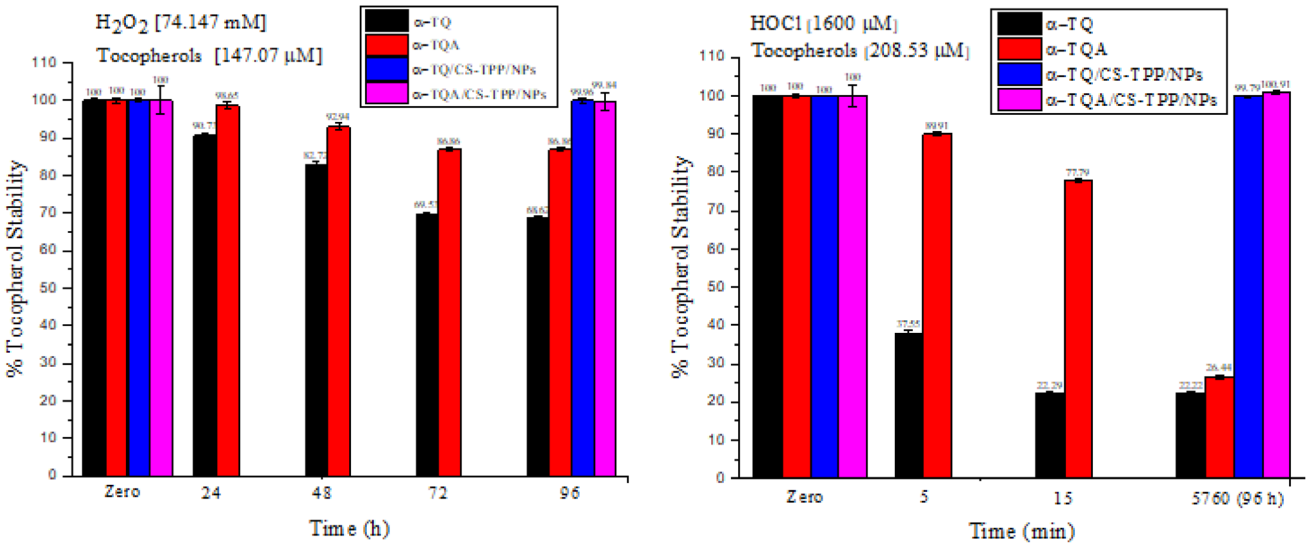

Fig. 6 Oxidative stability of nanoformulae (α-TQ/CS–TPP/NPs & α-TQA/CS-TPP/NPs) and their precursors (α-TQ & α-TQA) against H_2O_2 and HOCl. Results are means of triplicate, with error bars representing the standard deviations.

no reducing activity. This suggests that both hydrogen-atom and electron-donations require a free phenolic hydroxyl group. α-TQ/CS–TPP/NPs still displayed higher activity than α-TQ, particularly at elevated α-TQ concentrations.

3.6. Oxidative stability of α-tocopherols and their chitosan–TPP complex

Despite the crucial role of α-TQ in stabilizing fatty foods, it can be easily oxidized by various oxidants, making it essential to protect it in foods during storage and processing.[51] Consequently, the oxidative stability of α-TQ, α-TQA, and their nanoparticles was examined at H_2O_2/α-TQ concentrations of 74.15 mM/147.07 µM and HOCl/α-TQ concentrations of 1600/208.53 µM. The results (Fig. 6, Tables S7 and S8) indicated, as expected, that α-TQ exhibited lower stability (68.61%) compared to α-TQA (86.86%) under H_2O_2 conditions; stability was even lower under HOCl conditions (22.22% and 26.43%, respectively) after four days. Recently, we have identified the α-TQ oxidation products and proposed the oxidation mechanism.[52] Remarkably, however, the α-TQ nanoparticles maintained over 99.7% stability for four days, surpassing α-TQA and being similar to α-TQA–CS–TPP/NPs under both ROS conditions, highlighting the effectiveness of the CS/TPP encapsulation and nanoformulation in protecting α-TQ. Besides, nanoparticles of both α-TQ and α-TQA were preserved at 4 °C for 30 days without being affected (stability > 99%). Nanoemulsions of both tocopherol forms were also stored at 4 °C for 30 days, where they maintained their integrity without any visible aggregation.

3.7. Tocopherol release mechanism

The release of α-TQ and α-TQA from their chitosan–TPP complexes was examined using various models in two solvents, ethanol and methylene chloride, as presented in Fig. 5D. The figure shows that tocopherol release from both complexes was more complete in EtOH, reaching a maximum of 85.25% and 98.72% after 4320 min in EtOH than in CH_2Cl_2, 41.34% (420 min) and 34.85% (480 min), respectively. The release fits the first-order, Higuchi, and Hixson-Crowell models, with high R^2 values (R^2 > 0.979). The only exception is the release of both tocopherol forms in the non-polar solvent, methylene chloride, which gave relatively lower correlations with the first-order and Hixson-Crowell models (R^2 0.927–0.941) but still shows high Higuchi correlations (R^2 > 0.979).

Following first-order kinetics indicates that both α-TQ and α-TQA are dependent on the initial contents of their complexes; besides, they are released much faster in EtOH, with rate

Table 3 The α-TQ and α-TQA release parameters from their complexes in different solvents

		Model						
		1st order			Higuchi		Hixson–Crowell	
Complex	Solvent	k	$t_{0.5}$ (min)	R^2	k_H	R^2	k_{H-C}	R^2
α-TQ	EtOH	2.58×10^{-3}	268.60	0.996	0.1806	0.999	8.60×10^{-4}	0.996
	CH_2Cl_2	6.68×10^{-4}	1036.91	0.927	0.2731	0.979	2.23×10^{-4}	0.927
α-TQA	EtOH	2.90×10^{-3}	238.97	0.992	0.3938	0.984	9.67×10^{-4}	0.992
	CH_2Cl_2	8.23×10^{-4}	841.73	0.983	0.5875	0.983	2.74×10^{-4}	0.983

constants 3.86 and 3.52 times higher, and with shorter half-life periods in EtOH than in CH_2Cl_2, as presented in Table 3. This could be attributed to the potential formation of hydrogen bonds between EtOH as a solvent and both forms of tocopherol. The formation of hydrogen bonds between the tocopherols and the solvent (EtOH) is crucial for compensating for the loss of hydrogen bonds between the tocopherols and the chitosan–TPP in the complexes, thereby making the release of tocopherols more thermodynamically favorable. The release of the less polar acetate form, α-TQA, was slightly faster than that of α-TQ in both solvents, as expressed by a higher rate constant and shorter half-life period, which could be due to weaker binding to the chitosan–TPP host.

In addition, the high Higuchi correlations obtained in both solvents indicate that tocopherol release is diffusion-controlled, with higher Higuchi constants in EtOH. Correlation with the Hixson-Crowell model suggests that tocopherol release is accompanied by a decrease in particle size, possibly due to the high molecular size of tocopherols. Accordingly, the results indicate that tocopherols are released and diffuse more slowly in non-polar media, such as oils, than in more polar matrices, such as milk and certain cosmetics.

3.8. Oil thermo-oxidative stability by α-TQ and α-TQA nanoformulations

Lipid oxidation is the primary cause of food deterioration and represents a complex process that remains unresolved or unprevented. Therefore, controlling or suppressing it is essential for maintaining food quality, shelf-life, customer appeal, and economic value. Lipid oxidation is more pronounced in foods than in living organisms due to prolonged storage periods and exposure to high temperatures during cooking and

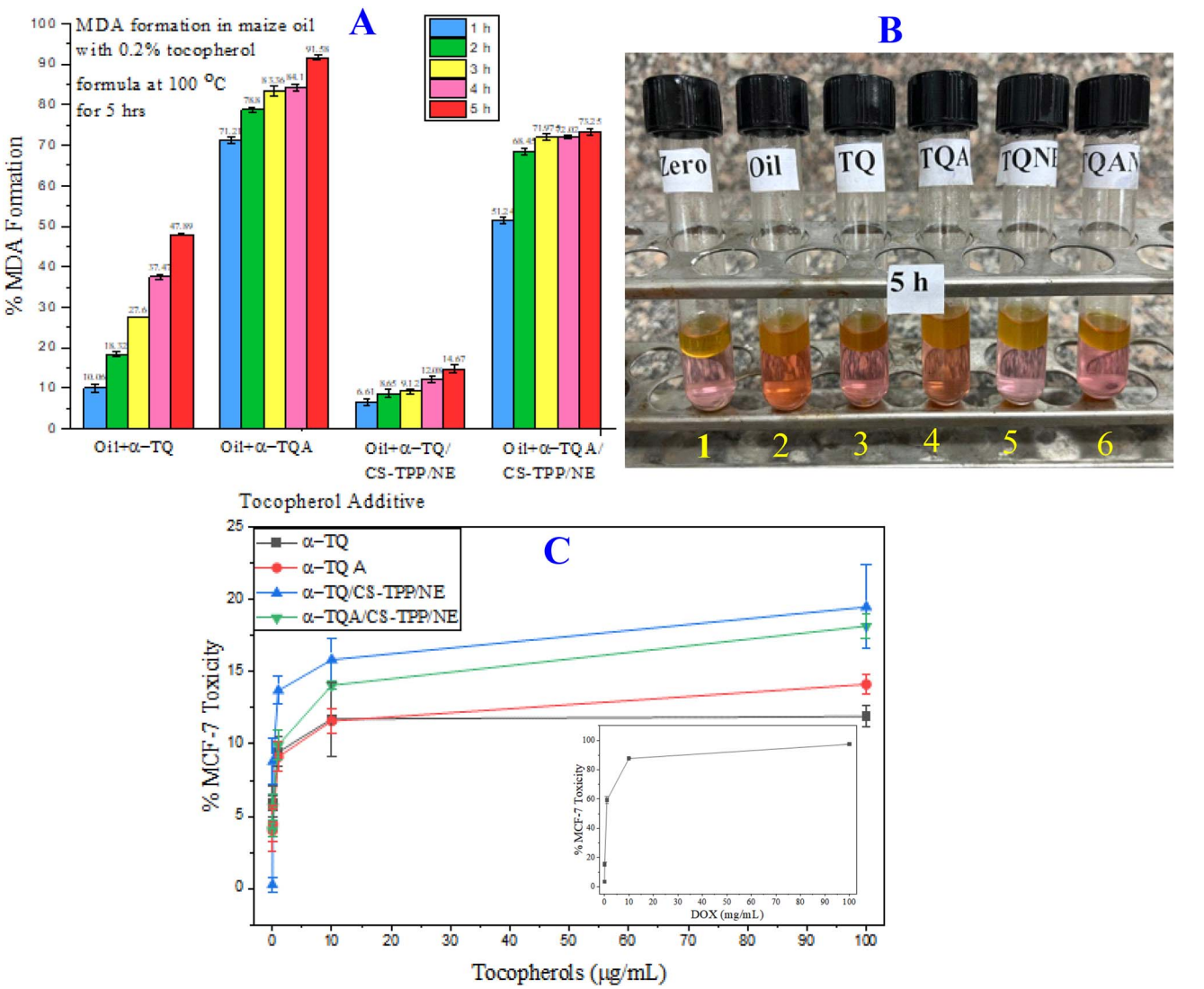

Fig. 7 (A) % of MDA formation of heated oils (5 h), relative to the unheated sample, with different tocopherol formulations. (B) MDA experiment tubes of (1) oil without heating, (2) heated oil, (3) heated oil + 0.2% α-TQ, (4) heated oil + 0.2% α-TQA, (5) heated oil + 0.2% α-TQ/CS–TPP/NE, and (6) heated oil + 0.2% α-TQA/CS–TPP/NE. Oil was heated at 100 °C for five hours before MDA determination. (C) Anticancer effects of tocopherol formulations and DOX (in a small window) on breast cancer (MCF-7) cells. Results are means of triplicate, with error bars representing the standard deviations.

frying.[53,54] Consequently, this study examined the control of lipid oxidation in maize oil at high temperature (100 °C) provided by the prepared tocopherol nanoemulsions (α-TQ/CS–TPP/NE and α-TQA/CS-TPP/NE).

α-TQA is commonly used as an oil stabilizer against oxidation in low concentrations (0.038–0.38%), typically at 0.2% but acts as a pro-oxidant at high concentrations (3.8%);[1,4] therefore, in this study, α-tocopherol forms were used in a concentration of 0.19% (w/v) either as free forms or in complexes. Fig. 7A and Table S9 show the MDA percentage formed in oils with different tocopherol formulas heated at various intervals (1–5 h) relative to the respective oil without additives. Results showed that α-TQ and its chitosan complex (α-TQ/CS–TPP/NE) are much more effective in reducing the oil oxidation than α-TQA and its complex (α-TQA/CS-TPP/NE). Furthermore, both complexes are better oil stabilizers than their precursors, α-TQ and α-TQA. These trends can be readily rationalized, as they match the trends in antioxidant activity (Section 3.5) and thermal stability (Section 3.3) of these formulas. For example, α-TQ/CS–TPP/NE expressed the highest antioxidant activity and thermal stability, where it exhibited superiority in preserving the oil oxidation state compared to other additives, as the %MDA did not exceed 14.7%, whereas the levels for other formulas ranged from 47.9% to 91.6% of the formed MDA in oil without additives at 100 °C for five hours (Table S9). Moreover, Fig. 7B also shows that α-TQ/CS–TPP/NE maintains the oil's appearance and color (tube 5) after five hours of heating at 100 °C, closely resembling the unheated oil (tube 1) in the MDA experiment. Encapsulation of antioxidants by various materials has been reviewed and found to modify oil stabilization.[55] It is worth noting that stabilizing oils against oxidation and preventing the formation of harmful products at high temperatures is crucial for preparing high-quality fried foods and reducing adverse effects on human health.

3.9. Anticancer activity of α-tocopherols and their nanoemulsions

Breast cancer is the most common cancer affecting women, accounting for 15.5% of cancer deaths among women worldwide.[56] The levels of α-TQ and α-TQQ in plasma were found to decrease in women who had cervical cancer.[57] The effects of tocopherol on breast cancer prevention are somewhat conflicting and not well documented,[58,59] and vary depending on the type of experiment, the animal used, the cell line, and the form of tocopherol. α-TQA and γ-TQ, but not α-TQ, showed a significant reduction in tumor volume in mice; α-TQ even exhibited an antagonistic effect, blocking the breast anticancer action of γ-TQ.[60] α-TQ reduced tumor volume by 19% *in vivo* in mice but had an insignificant effect on tumor weight or in the *in vitro* study.[61] α-TQA effectively reduced the survival of the murine breast cancer cell line 4T1.[62] Additionally, α-TQA reduced oxidative damage and enhanced breast tumor cell apoptosis in both *in vitro* and *in vivo* studies.[63] The inhibition of cancer cell proliferation by tocopherol is attributed to its potent antioxidant activity, which alleviates cellular oxidative stress and exhibits synergistic potential.[59]

The present work examined the anticancer effects of α-TQ and α-TQA, along with their nanoemulsions, on the breast MCF-7 cells. The results (Fig. 7C) showed that α-TQA had slightly greater cytotoxicity (14.1%) than α-TQ (11.9%) at 100 μg mL^{-1}, consistent with the findings of the *in vivo* experiment.[59] The potent anticancer drug Doxorubicin (DOX) showed much higher activity (97.5%). The nanoformulations of either α-TQ or α-TQA enhanced inhibition of breast cancer growth (19.5% and 18.2% cytotoxicity, respectively). Although the impact is not yet effective as a curing agent, the protective effect is improved by encapsulation and could be utilized as a dietary supplement or food additive for protective purposes. In addition, we have recently demonstrated that the α-TQ cytotoxicity against MCF-7 cells markedly increased at concentrations >200 μg mL^{-1}, reaching 77.7%,[52] suggesting that increasing the use of α-TQ could effectively reduce cancer risk.

4 Conclusion

Chitosan–TPP complexes of α-TQ and α-TQA were prepared and characterized. The former was optimized for minimum particle size, PDI, and maximum surface charge. Interestingly, the α-TQ/CS–TPP/NPs expressed higher thermal stability (436 °C) not only than that of α-TQ but also than α-TQA and its nanoparticles. Additionally, in contrast to both unencapsulated tocopherols, α-TQ/CS–TPP/NPs demonstrated much higher resistance (>99%) to hydrogen peroxide and hypochlorous acid. More importantly, α-TQ/CS–TPP/NPs exhibited even higher antioxidant activities than the original α-TQ against both DPPH and hydroxyl radicals, as well as higher reducing power. The kinetic release study revealed that the release of both α-TQ and α-TQA occurs more rapidly in a polar solvent and follows first-order, Higuchi, and Hixson-Crowell models, indicating that release is influenced by the initial tocopherol content and is primarily controlled by diffusion.

Applications of the developed nanoformulations as oil thermooxidative stabilizers and anticancer agents were examined. α-TQ/CS–TPP/NE exhibited significantly greater stability than both α-TQA and α-TQA/CS-TPP/NE, with only 14.7% MDA formed at 100 °C after five hours. Finally, α-TQA and α-TQA nanoemulsions improved their anticancer activity against the breast cancer cell line (MCF-7). Accordingly, the current results indicate that the prepared α-TQ/CS–TPP/NE offers better stabilization and activity than both α-TQ and α-TQA, making it a valuable option as a potent antioxidant, high-temperature oil stabilizer, and dietary supplement or food additive for anticancer protection.

The IC_{50} s of the tocopherols and their complexes for anticancer activity were not calculated because the used concentrations did not yield >20% activity. Future work could also examine the complex stability and antioxidant activity *in vivo* or in biological systems.

Author contributions

Hussein M. Ali: conceptualization, methodology, writing. Mohamed H. Attia: project administration, data curation. Wael

Mamdouh: conceptualization, administration, methodology, Eman N. Rashed: formal analysis, investigation, methodology. Isra H. Ali: formal analysis, investigation, writing.

Conflicts of interest

Authors disclose no financial or non-financial interests that are directly or indirectly related to the present publication. There are no competing interests among authors or with any other parties.

Abbreviations

α-TQ	α-Tocopherol
α-TQA	α-Tocopheryl acetate
CS	Chitosan
TPP	Tripolyphosphate
NE	Nanoemulsion
NPs	Nanoparticles
α-TQ/NE	α-Tocopherol nanoemulsion
α-TQA/NE	α-Tocopheryl acetate nanoemulsion
α-TQ/CS–TPP/NE	Nanoemulsion of α-tocopherol-chitosan-tripolyphosphate nanoemulsion
α-TQ/CS–TPP/NPs	Nanoparticles of α-tocopherol-chitosan-tripolyphosphate nanoparticles
α-TQA/CS-TPP/NE	Nanoemulsion of α-tocopheryl acetate-chitosan-tripolyphosphate nanoemulsion
α-TQA/CS-TPP/NPs	Nanoparticles of α-tocopheryl acetate-chitosan-tripolyphosphate nanoparticles
TEM	Transmission Electron Microscope
ROS	Reactive Oxygen Species
O/W	Octanol/Water
TBA	Thiobarbituric acid
TCA	Trichloroacetic acid

Data availability

All data used in this work are included in the manuscript.

Supplementary information (SI) is available. See DOI: https://doi.org/10.1039/d5ra06012e.

Acknowledgements

Open access funding provided by The Science, Technology & Innovation. Funding Authority (STDF) in cooperation with The Egyptian Knowledge Bank (EKB).

References

1 C. C. Chu, S. C. Chew, W. C. Liew and K. L. Nyam, Review article vitamin E: a multi-functional ingredient for health enhancement and food preservation, *J. Food Meas. Charact.*, 2023, **17**, 6144–6156, DOI: 10.1007/s11694-023-02042-z.

2 A. M. Rychter, S. Hryhorowicz, R. Słomski, A. Dobrowolska and I. Krela-Kaźmierczak, Antioxidant effects of vitamin E and risk of cardiovascular disease in women with obesity – a narrative review, *Clin. Nutr.*, 2022, **41**, 1557–1565, https://linkinghub.elsevier.com/retrieve/pii/S0261561422001510.

3 A. Azzi, Many tocopherols, one vitamin E, *Mol. Asp. Med.*, 2018, **61**, 92–103, DOI: 10.1016/j.mam.2017.06.004.

4 S. d. Caño-Ochoa, A. Ruiz-Aracama and M. D. Guillén, Alpha-tocopherol, a powerful molecule, leads to the formation of oxylipins in polyunsaturated oils differently to the temperature increase: a detailed study by proton nuclear magnetic resonance of walnut oil oxidation, *Antioxidants*, 2022, **11**, 604, https://www.mdpi.com/2076-3921/11/4/604.

5 H. M. Ali and I. H. Ali, QSAR and mechanisms of radical scavenging activity of phenolic and anilinic compounds using structural, electronic, kinetic, and thermodynamic parameters, *Med. Chem. Res.*, 2015, **24**, 987–998, DOI: 10.1007/s00044-014-1174-y.

6 H. M. Ali, M. H. Attia, K. M. A. Ramadan, E. N. Rashed and E. S. Bendary, Improving stabilization of α-tocopherol and α-tocopheryl acetate against oxidation, light and UV radiation by complexation with β-cyclodextrin and starch, *J. Food Sci. Technol.*, 2024, **62**, 75–87, DOI: 10.1007/s13197-024-06011-2.

7 W. C. Neely, J. M. Martin and S. A. Barker, Products and relative reaction rates of the oxidation of tocopherols with singlet molecular oxygen, *Photochem. Photobiol.*, 1988, **48**, 423–428, DOI: 10.1111/j.1751-1097.1988.tb02840.x.

8 M. Nishikimi, H. Yamada and K. Yagi, Oxidation by superoxide of tocopherols dispersed in aqueous media with deoxycholate, *Biochim. Biophys. Acta Gen. Subj.*, 1980, **627**, 101–108, DOI: 10.1016/0304-4165(80)90127-0.

9 K. Fukuzawa and J. M. Gebicki, Oxidation of α-tocopherol in micelles and liposomes by the hydroxyl, perhydroxyl, and superoxide free radicals, *Arch. Biochem. Biophys.*, 1983, **226**, 242–251, DOI: 10.1016/0003-9861(83)90290-4.

10 H. Botti, C. Batthyány, A. Trostchansky, R. Radi, B. A. Freeman and H. Rubbo, Peroxynitrite-mediated α-tocopherol oxidation in low-density lipoprotein: a mechanistic approach, *Free Radic. Biol. Med.*, 2004, **36**, 152–162, DOI: 10.1016/j.freeradbiomed.2003.10.006.

11 K. R. Duncan and Y. J. Suzuki, Vitamin E nicotinate, *Antioxidants*, 2017, **6**, 20, DOI: 10.3390/antiox6010020.

12 N. Smirnoff and D. Arnaud, Hydrogen peroxide metabolism and functions in plants, *New Phytol.*, 2019, **221**, 1197–1214, DOI: 10.1111/nph.15488.

13 C. K. Chow, W. Ibrahim, Z. Wei and A. C. Chan, Vitamin E regulates mitochondrial hydrogen peroxide generation, *Free Radic. Biol. Med.*, 1999, **27**, 580–587, DOI: 10.1016/S0891-5849(99)00121-5.

14 C. M. C. Andrés, J. M. P de la Lastra, C. A. Juan, F. J. Plou and E. Pérez-Lebeña, Hypochlorous acid chemistry in mammalian cells—influence on infection and role in various pathologies, *Int. J. Mol. Sci.*, 2022, **23**, 10735, DOI: 10.3390/ijms231810735.

15 G. Ozkan, P. Franco, I. De Marco, J. Xiao and E. Capanoglu, A review of microencapsulation methods for food antioxidants: Principles, advantages, drawbacks and

applications, *Food Chem.*, 2019, **272**, 494–506, DOI: 10.1016/j.foodchem.2018.07.205.

16 D. Wu, Y. Li, Y. Dai, H. Tian, Y. Chen, G. Shen and G. Yang, Stabilization of chitosan-based nanomedicines in cancer therapy: a review, *Int. J. Biol. Macromol.*, 2025, **309**, 143016, DOI: 10.1016/j.ijbiomac.2025.143016.

17 Y. Yang, M. Aghbashlo, V. K. Gupta, H. Amiri, J. Pan, M. Tabatabaei and A. Rajaei, Chitosan nanocarriers containing essential oils as a green strategy to improve the functional properties of chitosan: a review, *Int. J. Biol. Macromol.*, 2023, **236**, 123954, DOI: 10.1016/j.ijbiomac.2023.123954.

18 Y. Gao and Y. Wu, Recent advances of chitosan-based nanoparticles for biomedical and biotechnological applications, *Int. J. Biol. Macromol.*, 2022, **203**, 379–388, DOI: 10.1016/j.ijbiomac.2022.01.162.

19 S. Trombino, T. Poerio, F. Curcio, E. Piacentini and R. Cassano, Production of α-tocopherol–chitosan nanoparticles by membrane emulsification, *Molecules*, 2022, **27**, 2319, DOI: 10.3390/molecules27072319.

20 W. Yan, W. Chen, U. Muhammad, J. Zhang, H. Zhuang and G. Zhou, Preparation of α-tocopherol-chitosan nanoparticles/chitosan/montmorillonite film and the antioxidant efficiency on sliced dry-cured ham, *Food Control*, 2019, **104**, 132–138, DOI: 10.1016/j.foodcont.2019.04.026.

21 L. Zhang, Z. Liu, Y. Sun, X. Wang and L. Li, Effect of α-tocopherol antioxidant on rheological and physicochemical properties of chitosan/zein edible films, *LWT-Food Sci. Technol.*, 2020, **118**, 108799, DOI: 10.1016/j.lwt.2019.108799.

22 M. Heydari, A. Amirjani, M. Bagheri, I. Sharifian and Q. Sabahi, Eco-friendly pesticide based on peppermint oil nanoemulsion: preparation, physicochemical properties, and its aphicidal activity against cotton aphid, *Environ. Sci. Pollut. Res.*, 2020, **27**, 6667–6679, DOI: 10.1007/s11356-019-07332-y.

23 P. Mishra, B. K. Tyagi, N. Chandrasekaran and A. Mukherjee, Biological nanopesticides: a greener approach towards the mosquito vector control, *Environ. Sci. Pollut. Res.*, 2018, **25**, 10151–10163, DOI: 10.1007/s11356-017-9640-y.

24 L. Salvia-Trujillo, A. Rojas-Graü, R. Soliva-Fortuny and O. Martín-Belloso, Physicochemical characterization of lemongrass essential oil-alginate nanoemulsions: effect of ultrasound processing parameters, *Food Bioprocess Technol.*, 2013, **6**, 2439–2446, DOI: 10.1007/s11947-012-0881-y.

25 I. H. Ali, A. M. Elkashlan, M. A. Hammad and M. Hamdi, Antimicrobial and anti-SARS-CoV-2 activities of smart daclatasvir-chitosan/gelatin nanoparticles-in-PLLA nanofibrous medical textiles; in vitro, and in vivo study, *Int. J. Biol. Macromol.*, 2023, **253**, 127350, DOI: 10.1016/J.IJBIOMAC.2023.127350.

26 H. M. Ali, W. Almagribi and M. N. Al-Rashidi, Antiradical and reductant activities of anthocyanidins and anthocyanins, structure–activity relationship and synthesis, *Food Chem.*, 2016, **194**, 1275–1282, DOI: 10.1016/j.foodchem.2015.09.003.

27 W. Brand-Williams, M. E. Cuvelier and C. Berset, Use of a free radical method to evaluate antioxidant activity, *LWT-Food Sci. Technol.*, 1995, **28**, 25–30, https://linkinghub.elsevier.com/retrieve/pii/S0023643895800085.

28 N. Smirnoff and Q. J. Cumbes, Hydroxyl radical scavenging activity of compatible solutes, *Phytochem.*, 1989, **28**, 1057–1060, https://linkinghub.elsevier.com/retrieve/pii/0031942289801827.

29 M. Oyaizu, Studies on products of browning reaction: antioxidative activities of products of browning reaction prepared from glucosamine, *Japan J Nutr. Diet.*, 1986, **44**, 307–315, DOI: 10.5264/eiyogakuzashi.44.307.

30 P. Costa and J. M. S. Lobo, Modeling and comparison of dissolution profiles, *Eur. J. Pharm. Sci.*, 2001, **13**, 123–133, https://linkinghub.elsevier.com/retrieve/pii/S0928098701000951.

31 K. H. Ramteke, P. A. Dighe, A. R. Kharat and S. V. Patil, Mathematical models of drug dissolution: a review, Sch. Acad, *J. Pharm.*, 2014, **3**, 388–396.

32 S. Dash, P. N. Murthy, L. Nath and P. Chowdhury, Kinetic modeling on drug release from controlled drug delivery systems, *Acta Pol Pharm.*, 2010, **67**, 217–223.

33 M. Łukaszewicz, J. Szopa and A. Krasowska, Susceptibility of lipids from different flax cultivars to peroxidation and its lowering by added antioxidants, *Food Chem.*, 2004, **88**, 225–231, https://linkinghub.elsevier.com/retrieve/pii/S0308814604001062.

34 P. Skehan, R. Storeng, D. Scudiero, A. Monks, J. McMahon, D. Vistica, J. T. Warren, H. Bokesch, S. Kenney and M. R. Boyd, New colorimetric cytotoxicity assay for anticancer-drug screening, *J. Natl. Cancer Inst.*, 1990, **82**, 1107–1112, DOI: 10.1093/jnci/82.13.1107.

35 F. E. Hassan, B. E. Aboulhoda, I. H. Ali, H. M. Elwi, L. M. Matter, H. A. Abdallah, M. M. Khalifa, A. Selmy, M. A. Alghamdi, S. A. Morsy and B. A. Al Dreny, Evaluating the protective role of trimetazidine versus nano-trimetazidine in amelioration of bilateral renal ischemia/reperfusion induced neuro-degeneration: Implications of ERK1/2, JNK and Galectin-3/NF-κB/TNF-α/HMGB-1 signaling, *Tissue Cell*, 2023, **85**, 102241, DOI: 10.1016/j.tice.2023.102241.

36 W. K. Delan, I. H. Ali, M. Zakaria, B. Elsaadany, A. R. Fares, A. N. ElMeshad and W. Mamdouh, Investigating the bone regeneration activity of PVA nanofibers scaffolds loaded with simvastatin/chitosan nanoparticles in an induced bone defect rabbit model, *Int. J. Biol. Macromol.*, 2022, **222**, 2399–2413, DOI: 10.1016/j.ijbiomac.2022.10.026.

37 I. A. Khalil, I. H. Ali and I. M. El-Sherbiny, Noninvasive biodegradable nanoparticles-in-nanofibers single-dose ocular insert: in vitro, ex vivo and in vivo evaluation, *Nanomed*, 2019, **14**, 33–55, DOI: 10.2217/nnm-2018-0297.

38 S. Soleymanfallah, Z. Khoshkhoo, S. E Hosseini and M. H. Azizi, Preparation, physical properties, and evaluation of antioxidant capacity of aqueous grape extract loaded in chitosan-TPP nanoparticles, *Food Sci. Nutr.*, 2022, **10**, 3272–3281, DOI: 10.1002/fsn3.2891.

39 C. Lustriane, F. M. Dwivany, V. Suendo and M. Reza, Effect of chitosan and chitosan-nanoparticles on post harvest quality of banana fruits, *J. Plant Biotechnol.*, 2018, **45**, 36–44, DOI: 10.5010/JPB.2018.45.1.036.

40 E. N. Rashed, H. M. Ali, M. H. Attia, K. M. A. Ramadan and E. S. Bendary, Preparation and Thermal Stability of α-Tocopheryl acetate and Strawberry Anthocyanins Complexed with Starch and β-Cyclodextrin, *Arab Univ J Agric Sci*, 2021, **29**, 833–837, DOI: 10.21608/ajs.2021.91732.1408.

41 S. Selmi, Z. Limam, I. Batista, N. M. Bandarra and M. L. Nunes, Effects of storage temperature and α-tocopherol on oil recovered from sardine mince, *Int. J. Refrig.*, 2011, **34**, 1315–1322, https://linkinghub.elsevier.com/retrieve/pii/S0140700710002033.

42 E. Tabee, S. Azadmard-Damirchi, M. Jägerstad and P. C. Dutta, Effects of α-tocopherol on oxidative stability and phytosterol oxidation during heating in some regular and high-oleic vegetable oils, *J. Am. Oil Chem. Soc.*, 2008, **85**, 857–867, https://aocs.onlinelibrary.wiley.com/doi/10.1007/s11746-008-1274-2.

43 C. Diedrich, I. C. Zittlau, N. M. Khalil, A. F. G. Leontowich, R. A. Freitas, I. Badea and R. M. Mainardes, Optimized chitosan-based nanoemulsion improves luteolin release, *Pharmaceutics*, 2023, **15**, 1592, DOI: 10.3390/pharmaceutics15061592.

44 J. Hatanaka, H. Chikamori, H. Sato, S. Uchida, K. Debari, S. Onoue and S. Yamada, Physicochemical and pharmacological characterization of α-tocopherol-loaded nano-emulsion system, *Int. J. Pharm.*, 2010, **396**, 188–193, DOI: 10.1016/j.ijpharm.2010.06.017.

45 A. Shetta, I. H. Ali, N. S. Sharaf and W. Mamdouh, Review of strategic methods for encapsulating essential oils into chitosan nanosystems and their applications, *Int. J. Biol. Macromol.*, 2024, **259**, 129212, DOI: 10.1016/j.ijbiomac.2024.129212.

46 H. M. Ali and I. H. Ali, Energetic and electronic computation of the two-hydrogen atom donation process in catecholic and non-catecholic anthocyanidins, *Food Chem.*, 2018, **243**, 145–150, DOI: 10.1016/j.foodchem.2017.09.120.

47 A. A. Naiini, H. M. Ali Jr and C. H. Brubaker, Homogeneous selective hydrogenation of dienes and styrene derivatives by use of palladium ferrocenyl amine sulfide complexes as catalysts, *J. Mol. Catal.*, 1991, **67**, 47–56, http://www.sciencedirect.com/science/article/pii/030451029185033X.

48 J. T. Martins, M. A. Cerqueira and A. A. Vicente, Influence of α-tocopherol on physicochemical properties of chitosan-based films, *Food Hydrocoll.*, 2012, **27**, 220–227, DOI: 10.1016/j.foodhyd.2011.06.011.

49 H. M. Ali, A. Abo-Shady, H. A. Sharaf Eldeen, H. A. Soror, W. G. Shousha, O. A. Abdel-Barry and A. M. Saleh, Structural features, kinetics and SAR study of radical scavenging and antioxidant activities of phenolic and anilinic compounds, *Chem. Cent. J.*, 2013, **7**, 53–61, DOI: 10.1186/1752-153X-7-53.

50 A. Abaeea and A. Madadlou, Niosome-loaded cold-set whey protein hydrogels, *Food Chem.*, 2016, **196**, 106–113, DOI: 10.1016/j.foodchem.2015.09.037.

51 M. E. Player, H. J. Kim, H. O. Lee and D. B. Min, Stability of α-, γ-, or δ-tocopherol during soybean oil oxidation, *J. Food Sci.*, 2006, **71**, C456–C460, DOI: 10.1111/j.1750-3841.2006.00153.x.

52 H. M. Ali, M. H. Attia, W. Mamdouh, E. N. Rashed and I. H. Ali, Oxidative degradation of alpha-tocopherol by reactive oxygen species, identifying products, and product anticancer activity, *BMC Chem*, 2025, **19**, 306, DOI: 10.1186/s13065-025-01665-1.

53 D. Wang, H. Xiao, X. Lyu, H. Chen and F. Wei, Lipid oxidation in food science and nutritional health: a comprehensive review, *Oil Crop Sci.*, 2023, **8**, 35–44, DOI: 10.1016/j.ocsci.2023.02.002.

54 I. Bayram and E. A. Decker, Underlying mechanisms of synergistic antioxidant interactions during lipid oxidation, *Trends Food Sci. Technol.*, 2023, **133**, 219–230, DOI: 10.1016/j.tifs.2023.02.003.

55 G. L. Zabot, F. Schaefer Rodrigues, L. Polano Ody, M. Vinícius Tres, E. Herrera, H. Palacin, J. S. Córdova-Ramos, I. Best and L. Olivera-Montenegro, Encapsulation of bioactive compounds for food and agricultural applications, *Polymers*, 2022, **14**, 4194, DOI: 10.3390/polym14194194.

56 M. D. P. S. Sousa Coelho, I. C. Pereira, K. G. F. de Oliveira, I. K. F. Oliveira, M. d. S. Rizzo, V. A. de Oliveira, F. C. C. da Silva, F. L. Torres-Leal and J. M. de Castro e Sousa, Chemopreventive and anti-tumor potential of vitamin E in preclinical breast cancer studies: A systematic review, *Clin. Nutr. ESPEN.*, 2023, **53**, 60–73, https://linkinghub.elsevier.com/retrieve/pii/S2405457722005198.

57 P. R. Palan, A. L. Woodall, P. S. Anderson and M. S. Mikhail, α-Tocopherol and α-tocopheryl quinone levels in cervical intraepithelial neoplasia and cervical cancer, *Am. J. Obstet. Gynecol.*, 2004, **190**, 1407–1410, https://linkinghub.elsevier.com/retrieve/pii/S0002937804001528.

58 M. S. H. Ripon, M. A. Habib, M. Hossain, N. Ahmed, T. Kibria, S. Munira and K. Hasan, Role of vitamin E in prevention of breast cancer: an epidemiological review, *Asian J. Adv. Res. Rep.*, 2020, **11**, 37–47, https://journalajarr.com/index.php/AJARR/article/view/208.

59 R. Badraoui, M. Saeed, N. Bouali, W. S. Hamadou, S. Elkahoui, M. J. Alam, A. J. Siddiqui, M. Adnan, M. Saoudi and T. Rebai, Expression profiling of selected immune genes and trabecular microarchitecture in breast cancer skeletal metastases model: effect of α–tocopherol acetate supplementation, *Calcif. Tissue Int.*, 2022, **110**, 475–488, DOI: 10.1007/s00223-021-00931-3.

60 W. Yu, L. Jia, S.-K. Park, J. Li, A. Gopalan, M. Simmons-Menchaca, B. G. Sanders and K. Kline, Anticancer actions of natural and synthetic vitamin E forms: RRR-α-tocopherol blocks the anticancer actions of γ-tocopherol, *Mol. Nutr. Food Res.*, 2009, **53**, 1573–1581, DOI: 10.1002/mnfr.200900011.

61 M. J. Bak, S. Das Gupta, J. Wahler, H. J. Lee, X. Li, M.-J. Lee, C. S. Yang and N. Suh, Inhibitory effects of γ- and δ-tocopherols on estrogen-stimulated breast cancer in vitro and in vivo, *Cancer Prev. Res.*, 2017, **10**, 188–197, https://aacrjournals.org/cancerpreventionresearch/article/10/3/188/46555/Inhibitory-Effects-of-and-Tocopherols-on-Estrogen.

62 T. Hahn, L. Szabo, M. Gold, L. Ramanathapuram, L. H. Hurley and E. T. Akporiaye, Dietary administration of the proapoptotic vitamin E analogue α-Tocopheryloxyacetic acid inhibits metastatic murine breast cancer, *Cancer Res.*, 2006, **66**, 9374–9378, DOI: 10.1158/0008-5472.CAN-06-2403.

63 R. Badraoui, S. Blouin, M. F. Moreau, Y. Gallois, T. Rebai, Z. Sahnoun, M. Baslé and D. Chappard, Effect of alpha tocopherol acetate in Walker 256/B cells-induced oxidative damage in a rat model of breast cancer skeletal metastases, *Chem. Biol. Interact.*, 2009, **182**, 98–105, https://linkinghub.elsevier.com/retrieve/pii/S0009279709003913.